PHYSICAL REVIEW B VOLUME 39, NUMBER 13 1 MAY 1989

Pseudospin-phonon coupling model for martensitic transformation in bcc-based alloys

K. Fuchizaki and Y. Noda
Faculty of Engineering Science, Osaka University, Toyonaka-shi, Osaka 560, Japan

Y. Yamada
Institute for Solid State Physics, The University of Tokyo, 7-22-1 Roppongi, Minato-ku, Tokyo 106, Japan
(Received 28 November 1988)

We propose a new prescription to describe a general mechanism of the martensitic transformation in bcc-based alloys. We define a "three-state spin" variable which specifies local creation and annihilation of the "pseudospin" of the low-temperature phase and take into account the coupling of the spins to the lateral displacements of pseudospins thereby greatly reducing the degrees of freedom of the whole system. We obtain an effective Hamiltonian of the system given in terms of the pseudospin-creation energy and the pseudospin-pseudospin interaction energy via phonons. The phase-transition scheme is investigated based upon the model Hamiltonian. Overall characteristics of martensitic transformations including the premartensitic phenomena are successfully explained. Applications to the so-called 7*R* martensite in NiAl as well as premartensitic phenomena in AuCd are discussed.

I. INTRODUCTION

Many bcc metals (or β-type alloys) are known to undergo martensitic transformation,[1] a transformation from single phase to single phase without accompanying any atomic diffusion, at low temperatures. These metals have the following common characteristic features well established by x-ray, electron, and neutron diffraction experiments:[2-6] (1) Phonon dispersion curves show TA branches with a dip at $q=q_0$ ($q_0\neq 0$), a wave number characteristic of low-temperature phases, which slightly deepens with decreasing temperature. However, the frequencies of relevant phonon modes never tend to zero even at the transition temperature. (2) "Precursor" phenomena such as tweed patterns in electron micrograph and diffuse incommensurate spots in x-ray diffraction patterns have been observed well above the transition temperature. In spite of these experimental features and supplemental knowledge about certain crystallographic orientation relationships[7] between martensite phases and the parent phase, there has still been much controversy about a general microscopic description of these diffusionless phase transformations.

Recently, however, significant progress in understanding of the nature of martensite transformation has been made, in which all of the ideas are more or less based on the lattice instability against $\{110\}\langle 1\bar{1}0\rangle$ shear strains. Krumhansl[8] has claimed that, in contrast to the soft-mode mechanisms based on charge-density waves or Fermi-surface effects put forth by many authors, intrinsic bistable slow thermal fluctuations of the $\{110\}$ planes in $\langle 1\bar{1}0\rangle$ direction due to the extreme phonon anisotropy can just be the microscopic origin of the transformation. Clapp[9] and Guénin and Gobin[10] discussed the presence of stresses and strains around the impurities of the lattice which can induce a local mechanical instability against $\{110\}\langle 1\bar{1}0\rangle$ shear strains, thus leading to the "localized–soft-mode" concept. Later, this picture was incorporated[11] with the strain spinodal treatment developed by Suzuki and Wuttig[12] for martensitic transformations. Their treatment gives a possibility of the existence of "pseudospins" above the transition temperature induced around defects such as vacancies, interstitials, etc. A complete description comparable with experimental data is still lacking, however. The bcc lattice instability and its consequence to pretransformation morphologies are studied by Clapp *et al.*[13] by using a molecular-dynamics method to obtain "tweedlike" diffraction patterns.

With respect to those transient "precursor" phenomena Yamada *et al.*[14-16] have proposed the modulated-lattice-relaxation (MLR) model which was based on the dip in phonon dispersion mentioned above and the existence of thermally induced pseudospins, and have succeeded in explaining experimentally observed characteristics of the x-ray diffraction pattern in the TiNi(Fe) (Ref. 2) and AuCd.[3]

According to the MLR picture, the process of martensitic transformation is viewed as follows: at temperatures far above the transition temperature, pseudospins are frequently created by thermal excitation, but will soon be annihilated with a relaxation time $\tau_{ps}\sim e^{\Delta/k_BT}$, where Δ is an energy barrier height to form a pseudospin. Moreover, the pseudospin will stay "bare" because τ_{ps} is too short to induce the strain field around the pseudospins. As the temperature is lowered, so that the pseudospins become long lived, they can be "dressed," i.e., they can accompany the strain field around themselves. In the temperature range where pseudospin density is not still very high, the pseudospins are oriented randomly within equivalent directions satisfying cubic symmetry *on average*. This state may be identified to be the "premartensite" state. As the temperature is further decreased, the creation energy of the pseudospin will be decreased. At

the same time, interaction between pseudospins will become stronger, and eventually the whole lattice is cooperatively covered by the "ordered" pseudospins, which is nothing but the low-temperature phase. The transition temperature is well defined in view of the cooperative nature of the process.

The purpose of the present paper is to construct an appropriate model which is consistent with the picture described above, with specific applications to bcc (β) -martensite phase transformations. In the next section the model Hamiltonian is introduced, which is formulated so that the whole system is expressed effectively as a spin-phonon coupled system. In Sec. III the phase-transition scheme is discussed based on the model Hamiltonian. In particular, the quantities which characterize the pseudospin picture, such as pseudospin creation energy, pseudospin-pseudospin interaction, equilibrium pseudospin density, etc., will be discussed. In Sec. IV a case of practical importance, the bcc-7R transition, is treated as an application. The last section is devoted to summary and discussions.

II. MODEL HAMILTONIAN

To begin with, we explain our view using the example of the bcc (β) -9R transition, since most of the bcc-martensitic transformations belong to this class and the situation is simple enough to elucidate our idea.

The 9R structure is well established and considered to be deduced from the following two successive processes.[17]

(i) The symmetry change takes place due to small lattice distortion caused by a TA-phonon mode condensation with the wave vector $\mathbf{q}_0=\frac{1}{3}[110]$.

(ii) The distorted lattice is then deformed into the 9R type by introducing a macroscopic deformation, which is composed of the inclination of the [110] axis (Bain strain) and the elongation and contraction along the other two axes normal to the [110] axis, which construct the hexagonal basal plane.[18]

We can develop an alternative view to construct 9R structure as follows.

(i) Start from the small-amplitude phonon-condensed state with $\mathbf{q}_0=\frac{1}{3}[110]$ [see Fig. 1(a)].

(ii) Produce local fcc structure composed of three successive layers by increasing the amplitude of the condensed phonon and/or distorting the shape of the wave (or introducing higher harmonic waves) [Fig. 1(b)]. The parent lattice thus simulates *locally* the low-temperature structure. We refer to this local fcc structure as a "cluster."

(iii) Introduce an appropriate amount of slip at the boundaries between the local fcc structure along the $[1\bar{1}0]$ direction in order to relax the local stress [Figs. 1(b) and 1(c)]. Notice the relative atomic configuration at the cluster boundaries in Fig. 1(b) is definitely unstable.

These procedures [(i)–(iii)] result in the 9R structure [Fig. 1(c)].

This view is based on the assumption that the system has the tendency to form locally the fcc-type (ABC-type) stacking composed of at least three successive layers which acts as the pseudospin.

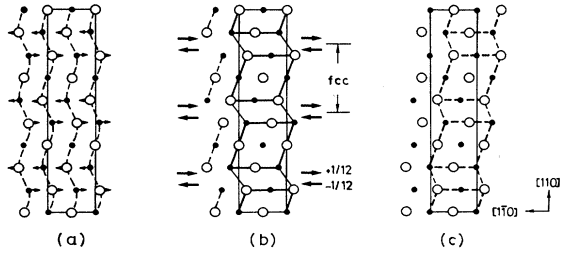

FIG. 1. Schematic illustration of the construction process of 9R martensite from a bcc (β) or a CsCl (β') lattice. In the following figures, the large open circles denote the A-type atoms on the plane of $z=0$ and small solid circles the B-type atoms on the plane of $z=\frac{1}{2}$. (a) Atomic arrangement in the condensed state of a TA phonon with $\mathbf{q}=\frac{1}{3}[110]$. Arrows indicate the further displacements of atoms introduced to form locally the fcc structure. (b) The chain of fcc "clusters" (enclosed by the thick lines) embedded in the resultant structure. Arrows indicate the relative slips of the cluster to take place at the cluster boundaries in the $[1\bar{1}0]$ direction. The amount of the relative displacement of the cluster due to the slip is $\frac{1}{6}$. (c) The resultant 9R structure. The same cluster chain as indicated in (b) is shown by the dashed lines. The rectangle enclosed by the solid line is the unit cell of the 9R structure.

Apart from the specific case of 9R, when the system is unstable against a phonon mode with $\mathbf{q}=\mathbf{q}_0$ along the [110] direction i.e., when the system has a dip in phonon dispersion at $\mathbf{q}_0$ along the [110] direction, the same view holds if the size of the pseudospin is taken appropriately. For later convenience, we describe the postulated shape of the pseudospin of the case for $\mathbf{q}_0=\frac{1}{7}[110]$ in Fig. 2.

If we consider, in general, that the cluster is the smallest unit with physical meaning associated with the phase-transition mechanism, the degree of the freedom of motion of the whole system under consideration can be reduced simply to the degree of freedom concerning the clusters; the translation of the center of mass of the clus-

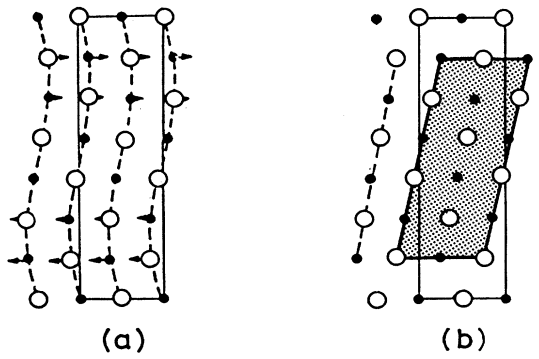

FIG. 2. Schematic illustration for the formation of the cluster (pseudospin) when $\mathbf{q}_0=\frac{1}{7}[110]$. (a) Dashed lines represent the small-amplitude phonon with $\mathbf{q}=\frac{1}{7}[110]$. Further displacements of atoms to form local fcc cluster are indicated by the arrows, which results in (b) a postulated cluster composed of six (110) layers (shown by the shadowed area).

ter along $[1\bar{1}0]$ and the shear deformation or the "tilt" of the cluster.

The first point to make is that there are two equivalent tilted states (see Fig. 3). Thus, together with the undeformed state the states of the cluster are represented by a "spin" variable with three eigenstates; $\sigma=(1,0,-1)$, among which $\sigma=\pm1$ are energetically degenerate by the symmetry of the parent (bcc) phase.[19]

In order to describe appropriately the strain energy stored at the cluster boundaries, both ends facing each other of the two consecutive clusters are connected by harmonic springs with spring constant κ (see Fig. 4). Let u_i be the lateral displacement (slip) of the ith cluster relative to the $(i-1)$th cluster. Furthermore, let u_i be equal to zero when two consecutive clusters are in high-temperature structure position. The energy associated with the cluster configuration can then be written as

$$U\{\sigma_i,u_i\}=\sum_i \tfrac{1}{2}\kappa u_i^2-\alpha u_i(\sigma_{i-1}+\sigma_i)\ ,\quad \alpha>0\ , \tag{1}$$

where the first term is simply an elastic energy. Note that in the second term the coefficient α represents the effect of coupling between $\{\sigma_i\}$ and $\{u_i\}$. The ground-state configuration for this interaction energy is easily seen to be $\sigma_i=-1$, $u_1=-2\alpha/\kappa$ or $\sigma_i=1$, $u_i=2\alpha/\kappa$ for all i. In addition, however, there is the contribution of creation energy ε associated with the local formation of the tilted cluster states. The origin of ε is more precisely understood by considering local potential energy $V_{\rm loc}$ of the cluster. As is shown in Fig. 5, we are considering that the local potential of the configuration of the cluster has "triple minimum" corresponding to the states $\sigma=1$, 0, or -1. The creation energy corresponds to the energy difference between $\sigma=0$ and $\sigma=\pm1$. Including this energy, our microscopic Hamiltonian is of the form

$$H\{\sigma_i,u_i\}=\sum_i \varepsilon\sigma_i^2+U\{\sigma_i,u_i\}\ . \tag{2}$$

Thus the cluster system is now expressed effectively by a (three-state) spin-phonon coupled system. The effects of the displacement field are readily renormalized through

$$e^{-\beta\tilde{H}\{\sigma_i\}}=\int d\{u_i\}e^{-\beta H\{\sigma_i,u_i\}},\quad \beta=1/k_BT\ , \tag{3}$$

to give an effective Hamiltonian $\tilde{H}\{\sigma_i\}$ of the spin system. $\tilde{H}\{\sigma_i\}$ thus obtained is, apart from a trivial part,

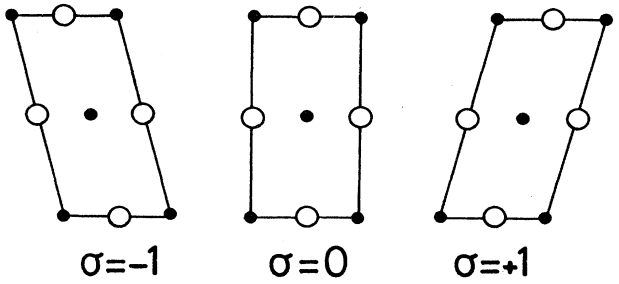

FIG. 3. Assignment of a spin variable to three-types of cluster states; $\sigma=0$ stands for the undeformed cluster state and $\sigma=\pm1$ for the tilted cluster states.

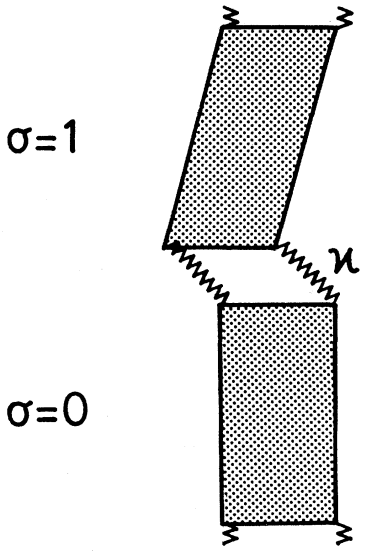

FIG. 4. Schematic illustration of the model composed of clusters (shaded region) connected by harmonic springs with spring constant κ. Only two consecutive clusters with states, for example, $\sigma=0$ and $\sigma=1$ are shown.

$$\tilde{H}\{\sigma_i\}=\sum_i \tilde{\varepsilon}\sigma_i^2-\tilde{J}\sigma_i\sigma_{i-1}\ , \tag{4}$$

where $\tilde{\varepsilon}$ and $\tilde{J}$ are the renormalized creation energy and the renormalized nearest-neighbor interaction between spins ("pseudospins"), respectively, and are given by

$$\tilde{\varepsilon}=\varepsilon-\alpha^2/\kappa\ , \tag{5a}$$

$$\tilde{J}=\alpha^2/\kappa\ . \tag{5b}$$

It should be noted that we are actually treating the ordering problem in three-dimensional space. In the final expression (4) σ_i means not a state of particular cluster in the one-dimensional (1D) cluster chain but an averaged quantity with respect to all spins in a plane which contains the ith cluster and is normal to the wave vector $\mathbf{q}_0$. Thus the parameters such as ε, α, and κ are not strictly of microscopic origin, but are semimacroscopic in the sense that they are associated with the statistical average within the layer.

III. PHASE-TRANSITION SCHEME

In order to discuss the phase transition from the high-temperature bcc phase, passing through the premartensitic state to the low-temperature martensite phase, we utilize the Hamiltonian obtained in the preceding section. The relevant quantities with which we are concerned are the cluster order parameter $\langle\sigma\rangle$, and the average amount of slip of a cluster $\langle u\rangle$. In addition, the quantity $\langle\sigma^2\rangle$ is of special interest here, because this quantity corresponds to the equilibrium pseudospin density which can be experimentally detected by quasielastic neutron scattering or diffuse x-ray scattering. In fact Noda *et al.*[3] have observed strong x-ray scattering in the premartensitic region in AuCd, and inferred that the low-temperature

pseudospins may exist with high density even above the transition temperature.

Before calculating the above quantities some attention must be paid to the temperature dependences of the parameters in the Hamiltonian. As is mentioned in the Introduction, phonons belonging to the [110]TA branch are weakly softened so that the spring constant κ may have a temperature dependence as $\kappa=\kappa_0(T-T_0)$ where T_0 is a fictitious critical temperature of intrinsic stability limit of the cubic phase which is far lower than the transition temperature. The creation energy ε of a single cluster can also be temperature dependent since we interpret ε as a semimacroscopic quantity. Going back to the local potential as depicted in Fig. 5, it would be quite reasonable to consider that ε is increasing with increasing temperature in order to be consistent with T dependence of κ, because κ is associated with the curvature of $V_{\rm loc}$ at $\sigma=0$, while ε is the energy difference of the minima of the same potential function. If this temperature dependence is given in a form of λT^{δ}, one can readily see that, from the equation in (6c) below, $\delta>1$ will be required since $\langle\sigma^2\rangle$ must vanish at temperatures far above the transition temperature. The precise choice of δ, however, is inessential for the equilibrium behaviors of $\langle\sigma\rangle$, $\langle u\rangle$, and also $\langle\sigma^2\rangle$ in the temperature region of interest. In fact, qualitatively the same results follow in our mean-field treatment for $\delta>1$. Here we have set $\delta=2$ rather arbitrarily.

To proceed, we use the mean-field approximation. Following the standard procedure, we have

$$\langle\sigma\rangle=\frac{2\sinh(\beta z\tilde{J}\langle\sigma\rangle)}{2\cosh(\beta z\tilde{J}\langle\sigma\rangle)+e^{\beta\varepsilon}}\ , \tag{6a}$$

$$\langle u\rangle=\frac{2\alpha}{\kappa}\langle\sigma\rangle\ , \tag{6b}$$

and

$$\langle\sigma^2\rangle=\frac{2\cosh(\beta z\tilde{J}\langle\sigma\rangle)}{2\cosh(\beta z\tilde{J}\langle\sigma\rangle)+e^{\beta\varepsilon}}\ , \tag{6c}$$

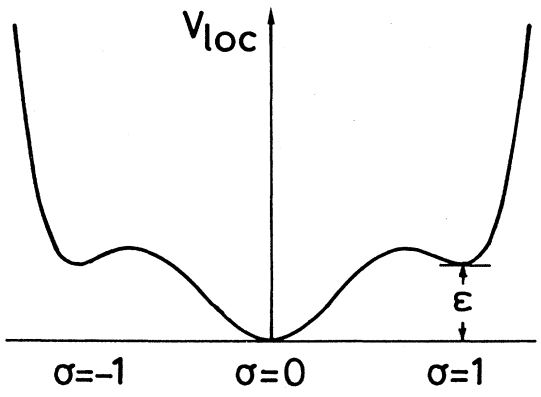

FIG. 5. Local potential $V_{\rm loc}$ having "triple minimum" corresponding to the states $\sigma=0,\pm1$. Note that states corresponding to $\sigma=\pm1$ are energetically degenerate. The difference of $V_{\rm loc}(\sigma=0)$ and $V_{\rm loc}(\sigma=\pm1)$ gives the creation energy of a single tilted cluster (a pseudospin of the low-temperature phase).

where z is the coordination number which is equal to 2 in our (pseudo) 1D system. We introduce a dimensionless temperature $\tau=\lambda T/k_B$ and a dimensionless parameter $\gamma=\lambda^2\alpha^2/\kappa_0 k_B^3$. One of the typical results is shown in Fig. 6 for the case of $\gamma=20$. Here we have set $T_0=0$ for simplicity. For this value of γ the first-order transition occurs at $\tau_c=3.389$. Below τ_c, the system exhibits cooperative ordering characterized by a nonzero value of $\langle\sigma\rangle$ and $\langle u\rangle$, which means that the martensite phase with the appropriate structure is stabilized below τ_c.

As is seen from Eq. (6b), $\langle u\rangle$ will tend to diverge as the temperature approaches T_0. This has resulted from the assumption of complete harmonicity of the springs which link spins (clusters) together. In real systems this intercluster interaction must have strong nonlinearity for such a large displacement that exceeds the amplitude of phonons, and at temperatures below τ_c this nonlinearity is considered to be responsible for the lock in of $\langle u\rangle$ to some value u_0.

In Fig. 6, it is noticeable that even above τ_c, where the system retains cubic symmetry, $\langle\sigma^2\rangle$ remains finite and slowly decays with increasing temperature as

$$\langle\sigma^2\rangle\propto e^{-\tau+\gamma/\tau^2}\ . \tag{7}$$

This feature is particularly important, because $\langle\sigma^2\rangle$ is proportional to the pseudospin density. The above feature justifies that under proper circumstances, there exists the equilibrium state where the low-temperature microstructures are distributed randomly with consider-

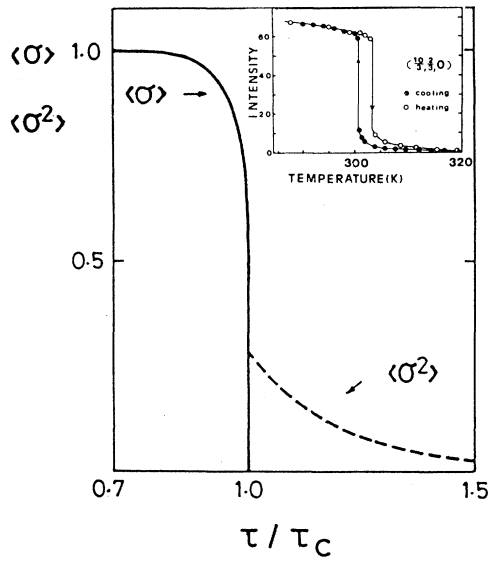

FIG. 6. The calculated variation of the order parameter $\langle\sigma\rangle$ (solid line) and of the pseudospin density $\langle\sigma^2\rangle$ (dashed line) with temperature. The abscissa is normalized by τ_c. Notice $\langle\sigma^2\rangle$ remains finite even above τ_c and gradually decreases as the temperature is increased. In the inset, the experimental result by the x-ray diffraction in Au-Cd (Ref. 3) is shown for comparison.

ably high density before the phase transition takes place. This temperature region, therefore, just corresponds to the premartensitic state. The Hamiltonian (4) thus satisfactorily describes the transition nature from the bcc phase to the martensite phase including the presence of premartensitic phenomena.

IV. APPLICATION TO NiAl

The low-temperature phase of NiAl is of special interest, since NiAl undergoes martensitic transformation[20] from high-temperature β phase to a particular $7R$-type structure. Extensive experimental studies show that this alloy has also the common features of martensitic transformations mentioned in Sec. I. In fact, phonon dispersion curves for the [110] $\langle 1\bar{1}0 \rangle$ TA_2 branch in Ni_xAl_{1-x} reveal a pronounced minimum at $q \sim 0.13$ ($x=0.63$),[5] whose position in the $\mathbf{q}$ space has concentration dependence, and substantial quasielastic scattering appears above the transition temperature. The intensity of the satellite reflections increases with decreasing temperature, and around $T \sim 253$ K, the crystal transforms to a martensite phase with a monoclinic unit cell.

Martynov *et al.*[21] studied the structures of the martensite phase by x-ray diffraction and proposed a specific structural model characterized by so-called (5-$\bar{2}$) stacking of successive hexagonal layers ($7R$ structure). Recently Shapiro *et al.*[22] performed detailed neutron diffraction measurements. They studied intensity profiles of the satellite peaks and reconfirmed the presence of superlattice reflections which are consistent with the $7R$ structure, except that the peak positions shift slightly from the commensurate positions of exact $7R$ periodicity. Schryvers *et al.*[23] also observed directly (5-$\bar{2}$)-type stacking by electron microscopy. It would be an interesting challenge to apply our model to this particular system.

Following the prescription described in Sec. II, we can construct the structure of the low-temperature (ordered) phase as follows. (i) Consider the small-amplitude TA-phonon-condensed state with $\mathbf{q}_0=\frac{1}{7}[110]$. (ii) Simulate locally the fcc structure by increasing the amplitude and deforming the shape of the wave [Fig. 7(a)]. In this case the pseudospin or the tilted cluster should be composed of six layers as has been postulated in Fig. 2(b). (iii) Introduce the boundary slips between the neighboring clusters [Figs. 7(b) and 7(c)]. As is illustrated in Fig. 7(c), this procedure in fact constructs qualitatively the (5-$\bar{2}$) structure. Notice that the resultant structure may be viewed as composed of alternative stacking of six-layer fcc slabs and three-layer distorted bcc slabs.

To be more quantitative, we allow the tilt angle θ of the fcc cluster to deviate slightly from the exact value to form the ideal fcc stacking ($\theta=71.57°$). This is related to the fact that in NiAl, the basal plane does not show complete hexagonality in the martensite phase.[24] In this context, our model structure may be expressed more exactly by the alternative stacking of (six-layer distorted fcc)–(three-layer distorted bcc). In the following analysis, we leave both the amount of slip u_0 and the tilted angle θ as parameters.

We now try to adjust the parameters so as to obtain

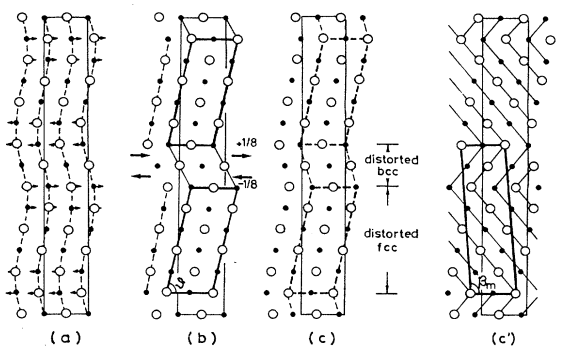

FIG. 7. Schematic illustration of the construction process of the martensite structure of NiAl. (a) See captions of Fig. 2. (b) Clusters are shown by the thick lines. Slips are introduced at the cluster boundaries in the directions indicated by the arrows. In this case the amount of the relative displacement due to the slip is $\frac{1}{4}$. (c) The resultant martensite structure, which is essentially identical to the so-called (5-$\bar{2}$) structure as is demonstrated in (c'). The rhomboid enclosed by the thick line in (c') is the monoclinic unit cell. Note that resultant structure is viewed as alternative stacking of a distorted fcc and a distorted bcc slabs. (See also the text.)

agreements with the experimental data. From the observed monoclinic angle, the value of u_0 is determined to be $u_0=0.250$. The tilt angle is then determined within a relevant range of θ ($71.57° \leq \theta \leq 90°$) so that the relative intensity of superlattice reflections is fitted to the observed profiles by neutron diffraction measurement. By taking $\theta=81.34°$, we obtained fairly good agreement along the $[\bar{2}+\zeta\, 2+\zeta\, 0]$ line. The comparison between

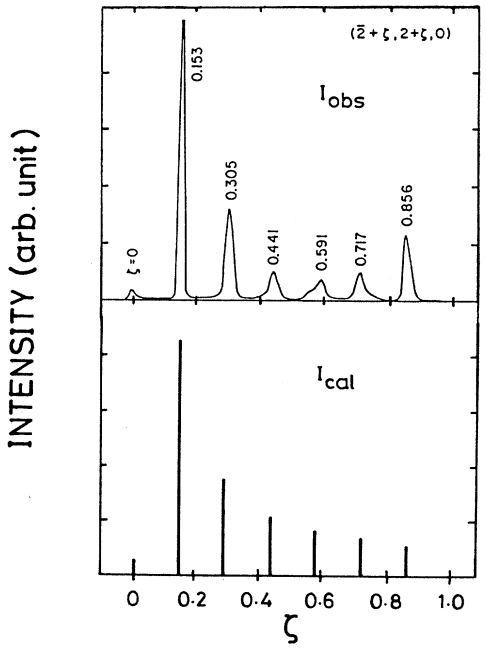

FIG. 8. Comparison between the calculated intensity profile (below) and the experimental results (Fig. 2 in Ref. 22).

the calculated intensity and the observed profile is given in Fig. 8. The obtained angle $\theta=81.34°$ is nearly equal to the corresponding angle $\theta=80.54°$ of the (5-$\bar{2}$) structure.

As far as the relative intensity is concerned, the results seem to be satisfactory. However, as stated above, the peak positions of experimental data are shifted from the commensurate position. This deviation apparently has no regularity either in magnitude or in direction. At the present stage, we are not able to give the theoretical basis of the shift pattern.

However, notice that we have considered the fully ordered ground-state configurations by taking $\langle\sigma\rangle=1$. It would be quite possible that, at finite temperatures, the positions of pseudospins, and hence the positions of "slips" are more or less randomly distributed along the [110] direction. This random configuration of pseudospins and slips may be the origin of Hendricks-Teller[25]-type irregularity of the diffraction pattern.

V. SUMMARY AND DISCUSSION

We summarize the results of the preceding sections as follows.

(i) We focus our attention upon the thermally induced pseudospins, which are considered to play an essential role in the martensitic transformation, and retain the degrees of freedom concerning the pseudospin motion by introducing a three-state spin variable σ. This leads to an effective Hamiltonian composed of two parts; the one stands for the creation energy of pseudospins and the other the interaction energy between pseudospins via phonons.

(ii) Using the Hamiltonian, the phase-transition scheme is investigated with the mean-field approximation to obtain the pseudospin order parameter $\langle\sigma\rangle$, the average amount of slip $\langle u\rangle$, and the equilibrium pseudospin density $\langle\sigma^2\rangle$. With a suitable choice of the parameters, a first-order transition takes place. Below the transition temperature, $\langle\sigma\rangle$ as well as $\langle u\rangle$ shows cooperative ordering, which correctly gives the martensite structure. On the other hand, $\langle\sigma^2\rangle$ is found to remain finite even above the transition temperature. This feature justifies the existence of the equilibrium state where the microstructure (pseudospins) of the low-temperature phase are distributed randomly within the parent phase, which is nothing but the premartensite phase.

(iii) We applied our model to interpret the low-temperature structure of NiAl. The so-called (5-$\bar{2}$) structure is reproduced as the "ordered state" with respect to σ and u. Qualitative agreements of the calculated intensity profile based on this model structure and the experimentally observed neutron intensity spectra are obtained.

In spite of the simplicity, our model seems to be able to explain primary features of the martensite transformation including premartensite behavior.

On the other hand, Gooding and Krumhansl[26] have treated the bcc-9R transition in Li from a different standpoint, in which the discussions are based upon the phenomenological Landau theory. In their free energy expansion, the uniform strain field e couples to the primary order parameter $\psi=Ae^{i(\mathbf{q}_0\cdot\mathbf{r}+\phi)}$ ($\mathbf{q}_0=\frac{1}{3}[110]$, $\mathbf{e}\|[1\bar{1}0]$) in the form $e\psi^3$. Much attention is paid to the ground-state solutions which minimize the free-energy functional and to the domain-wall structures when the Ginzburg-like term for the order parameter is included.

Recently, they have further extended the above theory to the NiAl case.[27] They specify the two independent order parameters; $\psi_1=A_1e^{i(\mathbf{q}_0\cdot\mathbf{r}+\phi_1)}$ and $\psi_2=A_2e^{i(2\mathbf{q}_0\cdot\mathbf{r}+\phi_2)}$, among which ψ_2 is *not* associated with any soft mode. The coupling to the uniform strain can then be described by the term $e\psi_1^2\psi_2^*$. They have obtained parameters to be fitted to the observed macroscopic strains. However, the values of A_1 and A_2 which should determine the relative displacement of each layer are left undetermined.

As far as the low-temperature structure is concerned, there would be no essential difference between the results obtained by Gooding and Krumhansl's treatments and the present "pseudospin ordering" picture. The difference is primarily seen in the premartensite phase. In the present treatment, the local variable σ_i is explicitly introduced. Hence, it seems to have the advantage of describing more naturally the pretransitional state in which the local symmetry has been already broken while the overall cubic symmetry is still retained.

Returning to our model, let us make some comments on our treatment. We have considered the ordering problem in one-dimensional space along a particular [110] axis by averaging out all fluctuations normal to this axis. As is pointed out in Ref. 19, there are six equivalent $\langle 110\rangle$ orientations, and there is no particular reason to regard a single [110] direction as a special one. In real materials, pseudospins should be oriented randomly in all equivalent directions. In fact, a "swirl" shift pattern of satellite peaks observed in NiTi(Fe) and AuCd are successfully explained by introducing pseudospins having two different orientations. Allowing the six possible $\langle 110\rangle$ orientations, the pseudospins should have the 12-fold degenerated excited states. We conjecture, however, that this will not cause any qualitative difference in the phase-transition scheme described in this paper.

Our Hamiltonian is still semimacroscopic in the sense that *ad hoc* temperature dependence of the pseudospin creation energy has been assumed. More microscopic basis is needed to understand the properties of the local potential $V_{\rm loc}$. In addition, anharmonicity for the displacement field must be taken into consideration to suppress the unphysical divergence as has been mentioned in Sec. III.

We make some remarks on the low-temperature structure of NiAl. As is mentioned in Sec. IV, we regard the amount of slip u_0 and the tilt angle θ as parameters; the former is determined by the observed monoclinic angle while the latter by comparing the calculated intensities with the experimental results in such a parameter range that $71.57°\leq\theta\leq 90°$. The (5-$\bar{2}$) structure is then almost uniquely determined in this parameter range. However, it is necessary for the complete understanding of the structure to investigate the satellite peak intensity profile

in many Brillouin zones. Once again we emphasize that we refer just to the ground-state configuration. Notice our standpoint is that the ground-state configuration results from the cooperating effect between pseudospins formed by *local* deformation or distortion. Hence it is rather likely that the system includes stacking faults (deformation and growth faults) at finite temperatures. The analyses performed by Berliner and Werner[28] will therefore be needed to explain precisely the experimentally observed diffraction patterns.

ACKNOWLEDGMENTS

The authors would like to express their sincere gratitude to Professor T. Ohta and H. Nozaki of Ochanomizu Women's University (Tokyo, Japan) for performing preliminary calculations for us. We also wish to thank Dr. S. M. Shapiro and Dr. G. Shirane of Brookhaven National Laboratory (Upton, NY) and Dr. L. E. Tanner of Lawrence Livermore National Laboratory (Berkeley, CA) for many fruitful discussions.

[1]The definitions of martensitic transformations are somewhat ambiguous. In this paper the term "martensitic transformation" refers to all types of diffusionless (or displacive in contrast to ordinary replacive) transformations.

[2]S. M. Shapiro, Y. Noda, Y. Fujii, and Y. Yamada, Phys. Rev. B **30**, 4314 (1984).

[3]Y. Noda, M. Takimoto, T. Nakagawa, and Y. Yamada, Metall. Trans. A **19**, 265(1988).

[4]M. Mori, Y. Yamada, and G. Shirane, Solid State Commun. **17**, 127(1975).

[5]S. M. Shapiro, J. Z. Larese, Y. Noda, S. C. Moss, and L. E. Tanner, Phys. Rev. Lett. **57**, 3199(1986).

[6]L. E. Tanner, A. R. Pelton, and R. Gronsky, J. Phys. (Paris) Colloq. **43**, C4-169 (1982).

[7]A. L. Roitburd, in *Solid State Physics,* edited by H. Ehrenreich, F. Seitz, and D. Turnbull (Academic, New York, 1978), Vol. 33, p. 317.

[8]J. A. Krumhansl, in *Nonlinearity in Condensed Matter,* Vol. 69 of *Springer Series in Solid-State Science,* edited by A. R. Bishop, D. K. Campbell, P. Kumar, and S. E. Trullinger (Springer-Verlag, Berlin, 1986), p. 255, and references therein.

[9]P. C. Clapp, Phys. Status Solidi B **57**, 561(1973).

[10]G. Guénin and P. F. Gobin, Metall. Trans. A **13**, 1127(1982).

[11]G. Guénin and P. C. Clapp, in *Proceedings of the International Conference on Martensitic Transformations,* ICOMAT-86 (Jap. Inst. Met., Sendai, 1987), p. 171.

[12]T. Suzuki and M. Wuttig, Acta Metall. **23**, 1069(1975).

[13]P. C. Clapp, J. Rifkin, J. Kenyon, and L. E. Tanner, Metall. Trans. A **19**, 783(1988).

[14]Y. Yamada, Y. Noda, M. Takimoto, and K. Furukawa, J. Phys. Soc. Jpn. **54**, 2940(1985).

[15]Y. Yamada, Y. Noda, and M. Takimoto, Solid State Commun. **55**, 1003(1985).

[16]Y. Yamada, Metall. Trans. A **19**, 777(1988).

[17]A. Nagasawa, J. Phys. Soc. Jpn. **40**, 1021(1976).

[18]Since the latter deformation is irrelevant for the later discussions, we just neglect this deformation hereafter.

[19]The degeneracy refers to that for the states with a fixed $\mathbf{q}_0$. Since there are six equivalent $\langle 110 \rangle$ orientations, the total degeneracy of a tilted cluster should be 12 in the real cubic system.

[20]J. L. Smialek and R. F. Hehemann, Metall. Trans. **4**, 1571(1973).

[21]V. V. Martynov, K. Enami, L. G. Khandros, S. Nenno, and A. V. Tkachenko, Phys. Met. Metallogr. (USSR) **55**, 136(1983).

[22]S. M. Shapiro, B. X. Yang, G. Shirane, Y. Noda, and L. E. Tanner, Phys. Rev. Lett. (to be published).

[23]D. Schryvers, L. E. Tanner, and S. M. Shapiro, in Proceedings of the MRS Symposium on "Shape Memory Materials" Inst. Mtg. Adv. Mtls. 88-89 (MRS, Pittsburgh, in press).

[24]According to the paper by Shapiro *et al.* (Ref. 22), the ratio γ of the principal axes a_m/b_m in the monoclinic a-b plane (pseudohexagonal basal plane) is given by $\gamma=1.54$. This value is just in between the ideal values for the bcc lattice ($\gamma=\sqrt{2}$) and the the fcc lattice ($\gamma=\sqrt{3}$). The observed monoclinic angle β_m is given as 94.37°.

[25]S. Hendricks and E. Teller, J. Chem. Phys. **10**, 147(1942).

[26]R. J. Gooding and J. A. Krumhansl, Phys. Rev. B **38**, 1695(1988).

[27]R. J. Gooding and J. A. Krumhansl Phys. Rev. B **39**, 1535(1989).

[28]R. Berliner and S. A. Werner, Phys. Rev. B **34** 3586(1986).